ARMY RESEARCH LABORATORY

Indentation Size Effect (ISE) of Transparent AlON and $MgAl_2O_4$

by Parimal J. Patel, Jeffrey J. Swab, Mark Staley, and George D. Quinn

ARL-TR-3852 **July 2006**

NOTICES

Disclaimers

The findings in this report are not to be construed as an official Department of the Army position unless so designated by other authorized documents.

Citation of manufacturer's or trade names does not constitute an official endorsement or approval of the use thereof.

Destroy this report when it is no longer needed. Do not return it to the originator.

Army Research Laboratory
Aberdeen Proving Ground, MD 21005-5069

ARL-TR-3852 **July 2006**

Indentation Size Effect (ISE) of Transparent AlON and $MgAl_2O_4$

Parimal J. Patel and Jeffrey J. Swab
Weapons and Materials Research Directorate, ARL

Mark Staley
Johns Hopkins University

George D. Quinn
National Institute of Standards and Technology

REPORT DOCUMENTATION PAGE

Form Approved
OMB No. 0704-0188

1. REPORT DATE *(DD-MM-YYYY)*	2. REPORT TYPE	3. DATES COVERED (From - To)
July 2006	Final	October 2000–September 2001

4. TITLE AND SUBTITLE
Indentation Size Effect (ISE) of Transparent AlON and $MgAl_2O_4$

5a. CONTRACT NUMBER

5b. GRANT NUMBER

5c. PROGRAM ELEMENT NUMBER

6. AUTHOR(S)
Parimal J. Patel, Jeffrey J. Swab, Mark Staley,[*] and George D. Quinn[†]

5d. PROJECT NUMBER
622105H84

5e. TASK NUMBER

5f. WORK UNIT NUMBER

7. PERFORMING ORGANIZATION NAME(S) AND ADDRESS(ES)
U.S. Army Research Laboratory
ATTN: AMSRD-ARL-WM-MD
Aberdeen Proving Ground, MD 21005-5069

8. PERFORMING ORGANIZATION REPORT NUMBER
ARL-TR-3852

9. SPONSORING/MONITORING AGENCY NAME(S) AND ADDRESS(ES)

10. SPONSOR/MONITOR'S ACRONYM(S)

11. SPONSOR/MONITOR'S REPORT NUMBER(S)

12. DISTRIBUTION/AVAILABILITY STATEMENT
Approved for public release; distribution is unlimited.

13. SUPPLEMENTARY NOTES
[*]Materials Science and Engineering Department, Johns Hopkins University, Baltimore, MD 21218
[†]Ceramics Division, National Institute of Standards and Technology, Gaithersburg, MD 20899

14. ABSTRACT
Hardness is a widely reported mechanical property for materials. Aluminum oxynitride (AlON) and magnesium aluminate spinel ($MgAl_2O_4$) are two important materials for some U.S. Army applications since they can be transparent in their polycrystalline form. In many of these military applications, harder materials tend to perform better, hence it is necessary to properly measure and compare hardness values of competing materials. Measuring the hardness of most ceramics is straightforward, but comparing the hardness data for different ceramics can be complicated due to the well-known indentation size effect (ISE). This report describes the determination of the Vickers hardness-load curves for transparent AlON and $MgAl_2O_4$ in a load range between 0.98 and 19 N. Both materials exhibited a significant decrease in hardness with increasing load. The critical hardness (the point at which fracture, rather than plastic deformation, is dominant around the indentation) of spinel and AlON was found to be 13.5 and 16.8 GPa, respectively, which differs from other investigations that did not take into account the ISE.

15. SUBJECT TERMS
hardness, transparent, ceramics, AlON, spinel

16. SECURITY CLASSIFICATION OF:			17. LIMITATION OF ABSTRACT	18. NUMBER OF PAGES	19a. NAME OF RESPONSIBLE PERSON
a. REPORT	b. ABSTRACT	c. THIS PAGE			Parimal J. Patel
UNCLASSIFIED	UNCLASSIFIED	UNCLASSIFIED	UL	20	19b. TELEPHONE NUMBER (*Include area code*) 410-306-0744

Contents

List of Figures

List of Tables

1. Introduction

Hardness characterizes the ceramic's resistance to deformation, densification, displacement, and fracture. Densification can be important since some microporosity is often present in sintered ceramics. Densification may also occur in some glasses. Microfracture and shear fracture under an indentation are also important deformation components. Hagan and Swain beautifully illustrate the complexity of the deformation, displacement, and fracture processes in a paper on fracture around indentations in glasses (*1*).

In recent years, there has been renewed interest in the indentation size effect (ISE) in brittle materials (*2–13*). The ISE in ceramics and glasses, wherein hardness decreases with increasing indentation load, occurs for both conventional Knoop and Vickers hardness but with slightly different trends. A constant hardness is typically reached at loads between 5 and 100 N, depending upon the material. Ideally, one should measure the entire hardness-load curve, but in practice, one reference or standard load is often chosen to facilitate comparisons between materials. Testers prefer to make the indentations as large as possible to reduce measurement uncertainties, yet not so large as to induce excessive cracking that interferes with the measurement or destroys the indentation altogether.

The use of a hard-face ceramic has been shown to improve the ballistic performance of systems under consideration for transparent armor and electromagnetic (EM) window applications (*14*). Transparent aluminum oxynitride (AlON) and magnesium aluminate spinel ($MgAl_2O_4$) are two materials of interest for these applications since both are harder than soda-lime-silica glass, the conventional transparent armor material, and they possess high elastic modulus, strength, and toughness, and low density. Additionally, in their polycrystalline forms, they can be transparent in the visible region through the mid-infrared region.

The development of models and parameters to predict ballistic behavior based on static material properties is a continuing effort. Currently LaSalvia (*15*) is developing a physically based model to correlate the effect of materials properties on ballistic data generated by Lundberg and Hauver (*16–18*). This new micromechanics model couples a wing-crack model (*19*) with the stress distribution developed by Hertz (*20*). It indicates that the most important material property is hardness followed by grain size and fracture toughness. Quinn and Quinn (*21*) have developed a brittleness parameter based on fracture energies and deformation ratios to account for the transition from deformation to fracture around hardness impressions with increase indentation loads. This index incorporates the hardness, elastic modulus, and fracture toughness of the material and may be a useful tool in screening ceramics for some applications.

While there are many hypotheses as to the importance of static properties as a predictor of ballistic performance, it is generally accepted that harder materials tend to provide better ballistic protection. Therefore, a reproducible means of measuring and comparing hardness values of different materials is needed. Since hardness is considered an important component of these models and parameters, it is the purpose of this report to examine and compare the Vickers hardness/load curves for AlON and $MgAl_2O_4$.

2. Experimental Procedure

2.1 Materials

AlON and $MgAl_2O_4$ were selected for this investigation. These materials have cubic crystal structures and can be transparent in a polycrystalline form. AlON has a transmission window of 0.2–5.5 μm and spinel has a window of 0.2–6 μm (*22*). The AlON material investigated was procured from Raytheon Corporation* and is marketed as Raytran. RCS Technologies produced the $MgAl_2O_4$† under a contract to the U.S. Army Research Laboratory (ARL), using a rate-controlled sintering schedule followed by hot isostatic pressing (HIPing). This material requires no sintering aids, resulting in a final product that is phase-pure stoichiometric spinel. Figure 1 illustrates the microstructure of both materials. The AlON is coarse-grained with a grain size between 150–200 μm (figure 1A). The grain boundaries are extremely clean and there are little, if any, secondary phases present. The presence of secondary phases such as porosity and impurities at the grain boundaries would be evident by a degradation of the optical properties. Spinel has a bimodal grain-size distribution with fine grains typically 5–20 μm in size (figure 1B) and very large grains on the order of 300 μm (figure 1C). The properties of these two materials have been previously measured as shown on table 1 (*23*).

2.2 Hardness Testing

The machine used for all hardness testing was a Wilson Tukon model 300 with a Vickers diamond indenter. The Tukon model 300 consists of an electronic filar unit for the measurement of the Vickers impression to within 0.5 μm. A calibration test was performed using a Wilson standard test block prior to the start of the testing series to verify the accuracy of the machine and the tester.

Results of the hardness testing on AlON and spinel are shown in table 2.

*Certain commercial equipment, instruments, or materials are identified in this report in order to specify the experimental procedure adequately. Such identification does not imply recommendation or endorsement by the U.S. Army Research Laboratory, nor does it imply that the materials are necessarily the best for the purpose.

†RCS Technologies, Inc., P.O. Box 12335, Research Triangle Park, NC 27709-2235.

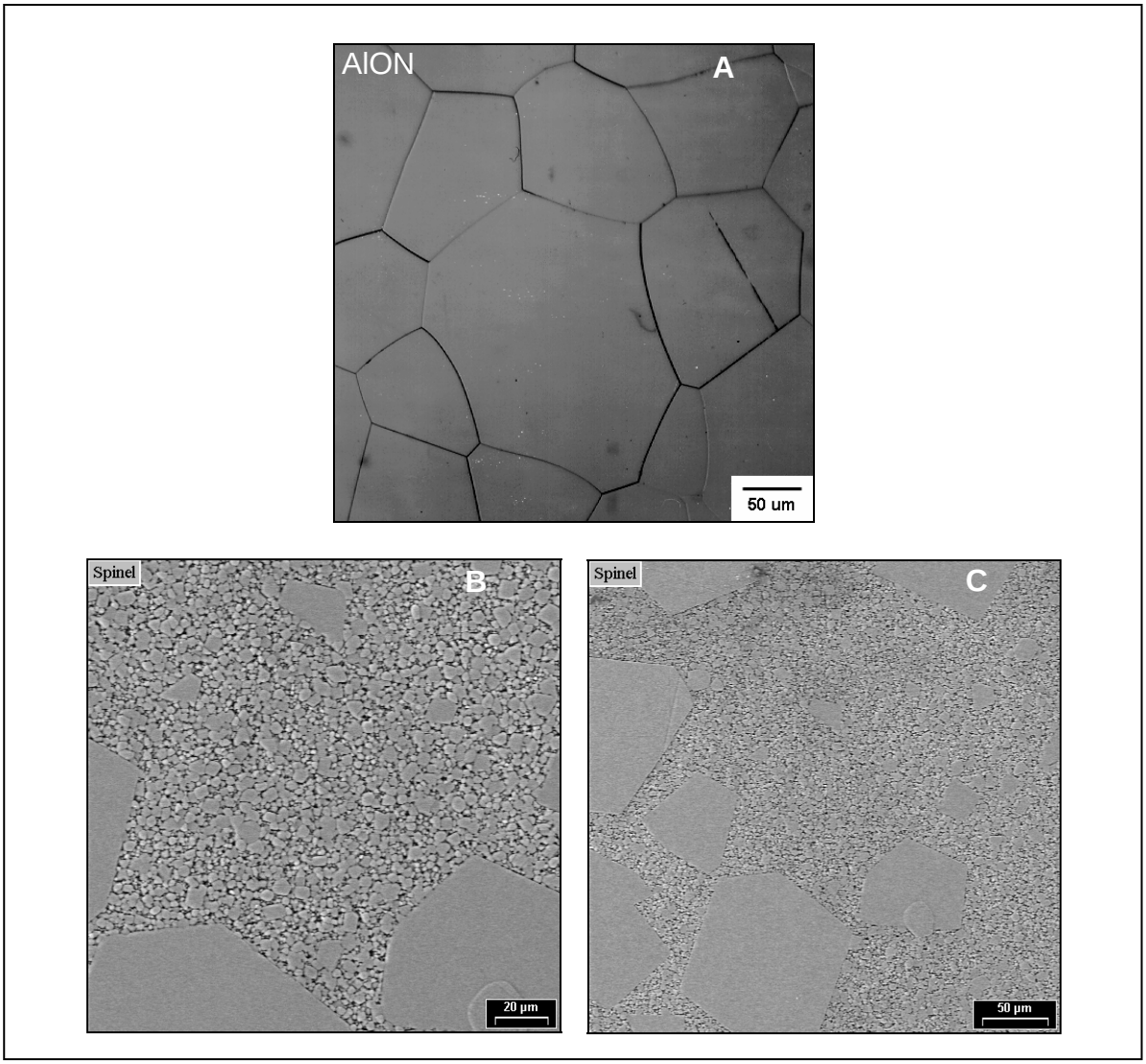

Figure 1. (A) Microstructure of the Raytheon Raytran aluminum oxynitride. Typical grains size of ~150–200 µm. (B and C) Microstructure of RCS technologies transparent spinel. Bimodal grain size distribution with fine grains typically 5–20 µm in size and large grains ~300 µm.

Table 1. Properties of Raytran aluminum oxynitride and RCS magnesium aluminate spinel (*23*).

Property	**Units**	**AlON**	**Spinel**
Density	g/cm^3	3.67	3.58
Elastic modulus (*24*)	GPa	315	277
Mean flexure strength (*25*)	MPa	228	241
Weibull modulus (*29*)	—	8.7	19.5
Fracture toughness (*26*)	$MPa\sqrt{m}$	2.40 ± 0.11	1.72 ± 0.06
Knoop hardness (HK_2) (*27*)	GPa	13.8 ± 0.3	12.1 ± 0.2

Table 2. Results of hardness testing on AlON and spinel. P_c was calculated by simultaneously solving two linear regression equations. H_c and d_c are measured values at the calculated P_c value.

Value	AlON	Spinel
H_c (GPa) measured	16.8 ± 0.4	13.5 ± 0.4
d_c (μm)	14.2	22.9
P_c (N)(calculated)	1.8	3.8
B (μm^{-1})	919	1263

Specimens were polished to an optical finish (0.25 μm). Five valid indentations were made at each load in a range between 0.98 N and 19.6 N for each material and averaged. Linear regression analysis was performed on two sets of data (low loads, high loads) to determine the transition load, P_c. The critical hardness, H_c for each material was then verified by conducting hardness tests at P_c.

Special precautions were taken with both materials to minimize errors. Since AlON has a large grained microstructure, indentations were only made within individual grains. Indentations were made only in the fine-grain region of the spinel since there was an insufficient number of large grains to complete the hardness study.

3. Results

3.1 Aluminum Oxynitride (AlON)

The Vickers hardness-load curve for aluminum oxynitride can be seen in figure 2. A linear regression analysis determined the transition load to be ~1.8 N with a corresponding calculated hardness of 16.2 GPa. Hardness measurements made at this transition load yielded a hardness value of 16.8 ± 0.4 GPa, well within the error for hardness measurements. For comparison, Raytheon has published* a Knoop hardness of 19.5 GPa with a 1.96-N load. The values are also significantly different from those generated for an aluminum oxynitride material produced by the U.S. Army in the early 1980s (*28*). The critical hardness of the older vintage was determined to be 14.6 GPa at a load of 7.6 N (*21*). The difference between these materials is in the microstructure.

The earlier version had a much finer grain size (~25μm) and contained micropores and porous zones that resulted in a lower density (3.61 g/cm^3) material. At loads below the transition point, cracking was predominately limited to cracks at the tips of the impressions with an occasional lateral crack. At the transition point, there was an increase in presence of lateral cracks, whose number increased with increasing loads.

*Raytheon product literature data.

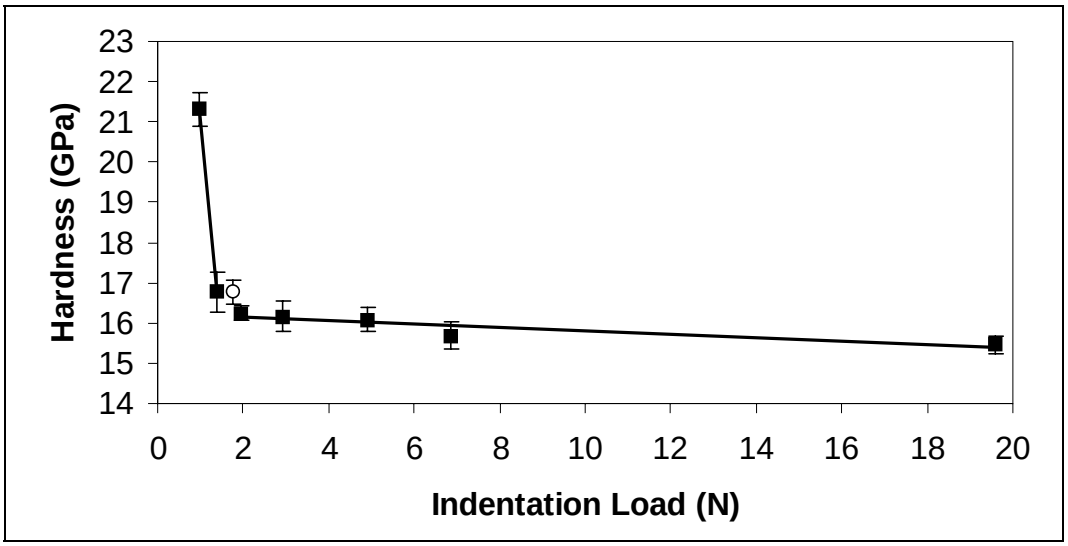

Figure 2. Hardness-load curve for aluminum oxynitride spinel. The open circle denotes the measured hardness measured at the calculated transition load (P_c).

3.2 Magnesium Aluminate Spinel ($MgAl_2O_4$)

Extensive lateral cracking was associated with the indents at all loads in this spinel. Reflections associated with this cracking made it difficult to accurately measure the size of the indentations. To obviate this problem, a 5-nm coating of gold-palladium was sputtered on to the spinel. The AlON did not require such a coating. To ensure that the coating did not affect the hardness values, measurements were made in coated and uncoated AlON. The results verify that this thin coating had a negligible effect on the resultant hardness values. Figure 3 shows the Vickers hardness-load curve for spinel. The calculated transition load is 3.8 N with a calculated hardness (H_c) of 13.9 GPa. Hardness measurements at 3.8 N yielded an H_c of 13.5 ± 0.4 GPa, again well within the error of the measurement.

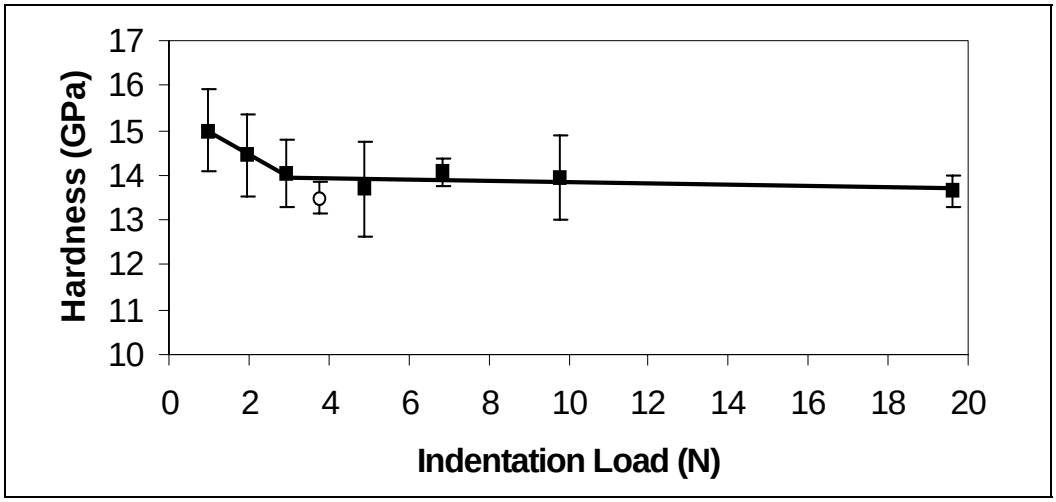

Figure 3. Hardness-load curve for magnesium aluminate spinel. Open circle denotes the measured hardness at the calculated transition load (P_c).

4. Discussion

The Vickers hardness-load curves for both AlON and $MgAl_2O_4$ showed an ISE between indentation loads of 0.98 and 19.0 N. AlON was determined to be 25% harder than spinel. The transition load was lower for AlON (1.8 N) than for spinel (3.8 N), resulting in AlON being almost 25% harder. This indicates the importance of determining a complete hardness-load curve for a material. The ISE in AlON is more pronounced than that for spinel. This may be due to the vastly different microstructures of each material. AlON is a course-grained material (>150 μm), with the grains being much larger than the size of the indentations. Since care was taken to indent only into individual grains, the hardness-load curve for AlON will be controlled by the properties of the individual grains (single-crystal properties) and the orientation of these grains to the indentation. On the other hand, the average grains in the spinel are significantly smaller than the indentations. Thus each indentation will sample many randomly oriented grains. This may account for the shallow hardness-load curve of the spinel. Associated with the observed ISE in AlON and spinel is a change in deformation mechanisms from primarily plastic deformation at low-indentation loads to one dominated by fracture at high-indentation loads (*29–31*). This fracture mode is not limited to one type of cracking but includes all cracking (cracking from the tips of the impression, lateral cracks, hidden subsurface cracking, etc.) due to the indentation process. This transition is the same as that seen by Quinn and Quinn (*21*) when they generated hardness/load curves using a Vickers indenter for a number of ceramic materials. They also observed an overlooked transition point that coincides with a similar shift in deformation mechanisms with increasing load. They defined the hardness at this transition point as the critical hardness (H_c) of the material. Based on these findings, a "brittleness parameter" (B, units of μm^{-1}) was introduced that describes the relationship between hardness and brittleness:

$$B \equiv \left(\frac{H_C E}{K_{Ic}^2} \right), \tag{1}$$

where E is the elastic modulus (GPa) and K_{Ic} is the fracture toughness (MPa$\sqrt{m}$) of the material. B is simply the ratio of indentation work (or work of deformation) to fracture energy (*21*). The implication of the ISE and its associated transition point is that hardness can no longer be simply compared for dissimilar (and maybe even similar) materials based solely on the same indenter type and indentation load. Instead, a full hardness/load curve should be generated for each material to ensure proper comparison.

A brittleness parameter was calculated for each material to gain insight between two potential transparent armor ceramics. The brittleness parameter for this AlON is 919 μm^{-1} vs. 618 μm^{-1} for an older vintage (lower-density, finer-grained) AlON (*21*). The brittleness parameter for this

spinel is 1263 μm^{-1}. The difference in the brittleness parameter between these materials agrees with observed damage around the indentations. Spinel has a wider load range where deformation rather than fracture is dominant around the indentations.

5. Conclusion

Vickers hardness-load curves were generated for transparent AlON and $MgAl_2O_4$ to investigate the indentation size effect in each material. Both materials exhibited ISE with the AlON having a more dramatic decrease in hardness with increasing load. The critical hardness was obtained from these plots and a brittleness parameter was calculated for each material. AlON was ~25% harder than spinel, but the spinel had a 37% higher brittleness parameter. The spinel has a wider load range (1–3.8 N) where deformation rather than fracture is dominant in the area immediately around the indentations. It appears that the brittleness parameter can be a useful value for comparing materials. However, care must be taken to ensure that the input (K_{Ic}, E, and H_c) values used to generate this parameter are appropriate for the material and its microstructure.

6. References

1. Hagan, J. T.; Swain, M. V. The Origin of Median and Lateral Cracks Around Plastic Indents in Brittle Materials. *J. Phys. D: Appl. Phys.* **1978**, *11*, 2091–2102.

2. Li, H.; Bradt, R. C. The Microhardness Indentation Size-Load Effect (ISE) in Hard Ceramic Materials. *J. Hard Mat.* **1992**, *3* (3–4), 403–419.

3. Li, H.; Bradt, R. C. The Effect of Indentation-Induced Cracking on the Apparent Microhardness. *J. Mat. Sci.* **1996**, *31*, 1065–1070.

4. Li, H.; Bradt, R. C. The Indentation Load/Size Effect and the Measurement of the Hardness of Vitreous Silica. *J. Non-Cryst. Sol.* **1992**, *146*, 197–212.

5. Sakai, T.; Ghosh, A.; Bradt, R. C. The Indentation Fracture Resistance of Self Reinforced Mullites. In *Fracture Mechanics of Ceramics*, Vol. 10; Bradt, R. C., et al., Eds.; Plenum: NY, 1992; pp 119–132.

6. Li, H.; Bradt, R. C. The Microhardness Indentation Load/Size Effect in Rutile and Cassiterite Single Crystals. *J. Mater. Sci.* **1993**, *28*, 917–926.

7. Li, H.; Ghosh, A.; Han, Y. H.; Bradt, R. C. The Frictional Component of the Indentation Size Effect in Low Hardness Testing. *J. Mater. Res.* **1993**, *8* (5), 1028–1032.

8. Swain, M.; Wittling, M. The Indentation Size Effect for Brittle Materials: Is There A Simple Fracture Mechanics Explanation. In *Fracture Mechanics of Ceramics*; Plenum: NY, 1996; pp 379–388.

9. Quinn, J. B.; Quinn, G. D. Indentation Brittleness of Ceramics: A Fresh Approach. *J. Mater. Sci.* **1997**, *32*, 4331–4346.

10. Yurkov, A. L.; Bradt, R. C. Load Dependence of Hardness of SIALON Based Ceramics. In *Fracture Mechanics of Ceramics*, Vol. 11; Bradt, R. C., et al., Eds.; Plenum: NY, 1996; pp 369–378.

11. Swain, M. V.; Wittling, M. Indentation Size Effects for Ceramics: Is there a Fracture Mechanics Explanation. In *Fracture Mechanics of Ceramics*, Vol. 11; Bradt, R. C., Hasselman, D. P. H., Munz, D., Sakai, M., Ya Shevchenko, V., Eds.; Plenum, New York, 1996; pp 379–387.

12. Sargent, P. M. ASTM STP 889. Use of the Indention Size Effect on Microhardness for Materials Characterization. In *Microindentation Techniques in Materials Science and Engineering*; Blau, P. J., Lawn, B. R., Eds.; ASTM: West Conshohocken, PA, 1986; pp 160–174.

13. Hirao, K.; Tomozawa, M. Microhardness of SiO_2 Glass in Various Environments. *J. Amer. Ceram. Soc.* **1987**, *70* (7), 497–502.

14. Patel, P. J.; Gilde, G. G.; Dehmer, P. G.; McCauley, J. W. Transparent Ceramics for Armor and EM Window Applications, PROC. SPIE Vol. 4102, *Inorganic Optical Materials II*, Marker, A. J., Arthurs, E. G., Eds.; October 2000, pp 1–14.

15. LaSalvia, J. C. A Physically-Based Model for the Effect of a Microstructure and Mechanical Properties on Ballistic Performance. In *Proceedings of 26th Annual International Conference on Advanced Ceramics & Composites*, Cocoa Bech, FL, 13–18 January 2002, in print.

16. Hauver, G. E.; Melani, A. Behaviour During Penetration of Long Rods (U). In *Proceedings of the Second BRL Topical Symposium: Experimental Research and Modeling Support*; U.S. Army Ballistic Research Laboratory: Aberdeen Proving Ground, MD, 24 May 1988; pp 149–160.

17. Hauver, G. E.; Netherwood, P. H.; Benck, R. F.; Kecskes, L. J. Ballistic Performance of Ceramic Targets. In *Proceedings of the 13th Army Symposium on Solid Mechanics*, Plymouth, MA, 17–19 August 1993; pp 23–34.

18. Hauver, G. E.; Netherwood, P. H.; Benck, R. F.; Rapacki, E. J. *Interface Defeat of Long Rod Projectiles by Ceramic Armor*. U.S. Army Research Laboratory: Aberdeen Proving Ground, MD, technical report in progress.

19. Hori, H.; Nemat-Nasser, S. Brittle Failure in Compression: Splitting, Faulting, and Brittle-Ductile Transition. *Phil. Trans. R. Soc. London A* **1986**, *319*, 337–374.

20. Lawn, B. R. Indentation of Ceramics With Spheres: A Century After Hertz. *J. Am. Ceram. Soc*. **1988**, *81* (8) 1977–94.

21. Quinn, J. B.; Quinn, G. D. Indentation Brittleness of Ceramics: A Fresh Approach. *J. Mat. Sci.* **1997**, *32*, 4331–4346.

22. Harris, D. C. Optical Properties of Window Materials. In *Infrared Window and Dome Materials*, edited by O'Shea, D. C.; SPIE: Bellingham, WA, 1992; p 40.

23. Swab, J. J.; LaSalvia, J. C.; Gilde, G. A.; Patel, P. J.; Motyka, M. J. Transparent Armor Ceramics: AlON and Spinel, *Ceram. Eng. Sci. Proc.* **1999**, *20* (4), 79–86.

24. ASTM C1259. Standard Test Method for Dynamic Young's Modulus, Shear Modulus, and Poisson's Ratio for Advanced Ceramics by Impulse Excitation. *Ann. Book of ASTM Stand.* **1998**, Vol. 15.01.

25. ASTM C1161. Standard Test Method for Flexural Strength of Advanced Ceramics at Ambient Temperatures. *Ann. Book of ASTM Stand.* **1998**, Vol. 15.01.

26. ASTM C1421-99. Standard Test Methods for the Determination of Fracture Toughness of Advanced Ceramics at Ambient Temperatures. To be published in the *Ann. Book of ASTM Stand.* **1999**, Vol. 15.01.

27. ASTM C1326-96a. Standard Test Method for Knoop Indentation Hardness of Advanced Ceramics. *Ann. Book of ASTM Stand.* **1998**, Vol. 15.01.

28. Quinn, G. D.; Corbin, N. D.; McCauley, J. W. Thermomechanical Properties of Aluminum Oxynitride Spinel. *Am. Ceram. Soc. Bull.* **1984**, *63* (5), 723–730.

29. Lawn, B. R.; Marshall, D. B. Hardness, Toughness, and Brittleness: An Indentation Analysis. *J. Am. Ceram. Soc.* **1979**, *62*, 347–350.

30. Lawn, B. R.; Evans, A. G. A Model for Crack Initiation in Elastic/Plastic Indentation Fields. *J. Mater. Sci* **1977**, *12*, 2195–2199.

31. Lawn, B. R.; Jensen, T.; Arora, A. Brittleness as an Indentation Size Effect. *J. Mater. Sci. Letters* **1976**, *11*, 573–575.

NO. OF COPIES	ORGANIZATION
1 (PDF ONLY)	DEFENSE TECHNICAL INFORMATION CTR DTIC OCA 8725 JOHN J KINGMAN RD STE 0944 FORT BELVOIR VA 22060-6218
1	US ARMY RSRCH DEV & ENGRG CMD SYSTEMS OF SYSTEMS INTEGRATION AMSRD SS T 6000 6TH ST STE 100 FORT BELVOIR VA 22060-5608
1	INST FOR ADVNCD TCHNLGY THE UNIV OF TEXAS AT AUSTIN 3925 W BRAKER LN AUSTIN TX 78759-5316
1	DIRECTOR US ARMY RESEARCH LAB IMNE ALC IMS 2800 POWDER MILL RD ADELPHI MD 20783-1197
3	DIRECTOR US ARMY RESEARCH LAB AMSRD ARL CI OK TL 2800 POWDER MILL RD ADELPHI MD 20783-1197

ABERDEEN PROVING GROUND

1	DIR USARL AMSRD ARL CI OK TP (BLDG 4600)

NO. OF COPIES ORGANIZATION

2 US ARMY RESEARCH OFC
J CHANG
D STEPP
PO BOX 12211
RESEARCH TRIANGLE PARK NC
27709-2211

4 DARPA
TACTICAL TECH OFC
W JOHNSON
DEFENSE SCIENCE OFC
L CHRISTODOULOU
S WAX
ADV TECH OFC
D HONEY
3701 N FAIRFAX DR
ARLINGTON VA 22203-1714

1 COMMANDER
AMSTA TAR R
D TEMPLETON
6501 E ELEVEN MILE RD
WARREN MI 48697-5000

1 COMMANDER
AMSTA JSK
L FRANKS
6501 E ELEVEN MILE RD
WARREN MI 48697-5000

1 COMMANDER
US ARMY TACOM
PM COMBAT SYS
SFAE GCS CS
6501 ELEVEN MILE RD
WARREN MI 48397-5000

1 COMMANDER
US ARMY TACOM
AMSTA SF
WARREN MI 48397-5000

1 COMMANDER
US ARMY TACOM
PM SURV SYS
SFAE ASM SS
6501 ELEVEN MILE RD
WARREN MI 48397-5000

1 COMMANDER
US ARMY AMCOM
AVIATION APPLIED TECH DIR
J SCHUCK
FORT EUSTIS VA 23604-5577

NO. OF COPIES ORGANIZATION

1 COMMANDER
US ARMY TACOM
PEO CS & CSS
PM LTV
SFAE CSS LT (M114 MGR)
6501 ELEVEN MILE RD
WARREN MI 48397-5000

1 COMMANDER
NSWC
CARDEROCK DIV
R PETERSON CODE 2020
BETHESDA MD 20084

1 USARDEC
AVIATION AND MISSILE RESEARCH
DEV & ENGRNG CTR
AMSRD AMR PS WF
A MCDONALD
REDSTONE ARSENAL AL 35898

1 NAVAL AIR WARFARE CTR
CHEMISTRY BRANCH
WEAPONS DIV CODE 4.9.8.2.0.0.D
R SULLIVAN
1900 N KNOX RD STOP 6303
CHINA LAKE CA 93555-6100

1 MATERIALS ENGRNG
RAYTHEON IDS ANF B16
SR MGR ENGRNG
R GENTILMAN
350 LOWELL ST
ANDOVER MA 01810

1 OAK RIDGE NATL LAB
1 BETHEL VALLEY RD
WERESZCZAK
PO BOX 2008
BLDG 4515 MS 6068
OAK RIDGE TN 37831-6068

4 SOUTHWEST RESEARCH INST
SECURITY OFC
C ANDERSON
J WALKER
K DANNEMAN
M SMITH
718 FOURTH ST MS 6100
ARNOLD AFB TN 37389-6100

NO. OF
COPIES ORGANIZATION

1 SANDIA NATL LAB
LALIT SOLID DYNAMICS &
ENERGETIC MATERIALS DEPT
DEPT 1647 MS1181
C CHHABILDAS
ALBUQUERQUE NM
87185-1181

3 SURMET CORP
L GOLDMAN
J WAHL
T HARTNETT
33 B ST
BURLINGTON MA 01803

2 TECH ASSESSMENT & TRANSFER
A DIGIOVANNI
L FEHRENBACHER
215 NAJOLES RD UNIT C
MILLERSVILLE MD 21108

1 NAVAL AIR SYSTEMS COMMAND
D HARRIS
CODE 498200D
1900 N KNOX RD STOP 6303
CHINA LAKE CA 93555-6106

1 US ARMY RDECOM
RESEARCH OPTICAL ENGR
AMSRD AMR WS PL
J KIRSCH
REDSTONE ARSENAL AL 35898-5000

1 NATL INSTITUTE OF STANDARDS
AND TECH
CERAMICS DIV BLDG 223 STOP 8520
G QUINN
GAITHERSBURG MD 20899-8520

ABERDEEN PROVING GROUND

19 DIR USARL
AMSRD ARL WM
J LASALVIA
J MCCAULEY
S MCKNIGHT
J SMITH
AMSRD ARL WM MB
J SWAB (5 CPS)
AMSRD ARL WM MD
P PATEL (10 CPS)

INTENTIONALLY LEFT BLANK.